Appl Microbiol Biotechnol (2012) 93:1637–1650
DOI 10.1007/s00253-011-3526-6

Primary metabolism in the new human cell line AGE1.HN at various substrate levels: increased metabolic efficiency and α_1-antitrypsin production at reduced pyruvate load

Jens Niklas · Christian Priesnitz · Thomas Rose · Volker Sandig · Elmar Heinzle

Received: 30 May 2011 / Revised: 20 July 2011 / Accepted: 3 August 2011 / Published online: 14 August 2011

Abstract Metabolic responses of the new neuronal human cell line AGE1.HN to various substrate levels were analyzed in this study showing that reduced substrate and especially pyruvate load improves metabolic efficiency, leading to improved growth and α_1-antitrypsin (A1AT) production. The adaptation of the metabolism to different pyruvate and glutamine concentrations was analyzed in detail using a full factorial design. The most important finding was an increasingly inefficient use of substrates as well as the reduction of cell proliferation with increasing pyruvate concentrations in the medium. Cultivations with different feeding profiles showed that the highest viable cell density and A1AT concentration (167% of batch) was reached in the culture with the lowest glucose level and without pyruvate feeding. Analysis of metabolic fluxes in the differently fed cultures revealed a more efficient metabolic phenotype in the cultures without pyruvate feeding. The measured in vitro enzyme activities of the selected enzymes involved in pyruvate metabolism were lower in AGE1.HN compared with CHO cells, which might explain the higher sensitivity and different adaptation of AGE1.HN to increased pyruvate concentrations. The results indicate on the one hand that increasing the connectivity between glycolysis and the TCA cycle might improve substrate use and, finally, the production of A1AT. On the other hand, a better balanced substrate uptake promises a reduction of energy spilling which is increased with increasing substrate levels in this cell line. Overall, the results of this study provide important insights into the regulation of primary metabolism and into the adaptation of AGE1.HN to different substrate levels, providing guidance for further optimization of production cell lines and applied process conditions.

Keywords Mammalian cell · Human cell · Metabolic flux · Recombinant protein · CHO · Physiology

Introduction

Mammalian cells represent nowadays the predominant system for the production of recombinant proteins for clinical applications because of their ability to secrete properly folded and glycosylated proteins. Around 70% of recombinant therapeutic proteins are produced using cell culture processes, and this number is further increasing (O'Callaghan and James 2008). Intensive research in the past led to enormous improvement of the performance of mammalian cells (Wurm 2004). This was mainly enabled through better understanding and modification of the parameters that influence productivity like cell growth, gene expression (Korke et al. 2004), metabolism (Bonarius et al. 2001; Cruz et al. 1999), protein secretion (Omasa et al. 2008), or repression of apoptosis (al-Rubeai and Singh 1998; Arden and Betenbaugh 2006; Nivitchanyong et al. 2007). For specific therapeutic glycoproteins with complex glycosylation, human cell lines may have an advantage compared to animal-derived cell lines since these human cells have a genuine human glycosylation system. The

Electronic supplementary material The online version of this article (doi:10.1007/s00253-011-3526-6) contains supplementary material, which is available to authorized users.

J. Niklas · C. Priesnitz · E. Heinzle (✉)
Biochemical Engineering Institute, Saarland University,
66123 Saarbrücken, Germany
e-mail: e.heinzle@mx.uni-saarland.de

T. Rose · V. Sandig
ProBioGen AG,
13086 Berlin, Germany

engineered cell line AGE1.HN represents such a very promising human-derived production system. In some initial studies, it was shown that these cells are well suitable for the production of complex glycoproteins (Blanchard et al. 2011).

The neutrophil elastase inhibitor α_1-antitrypsin (A1AT) represents a glycoprotein requiring *N*-glycosylation at three sites (Carrell et al. 1981). In the clinic, A1AT is required to treat patients having A1AT deficiency, an inherited disease that can result in lung emphysema and liver dysfunction (Petrache et al. 2009; Kelly et al. 2010). Patients with lung disease can be treated with A1AT augmentation therapy decreasing the mortality risk (A1AT-Group 1998). In spite of the fact that recombinant A1AT was produced in different prokaryotic and eukaryotic expression systems, there are currently only plasma-derived products licensed by the US FDA for intravenous treatment of A1AT deficiency (Karnaukhova et al. 2006). An alternative source for A1AT would be highly desirable since A1AT augmentation therapy is currently very expensive and not cost-effective (Gildea et al. 2003). A1AT derived from AGE1.HN cell has similar anti-inflammatory activity as the commercial A1AT from human plasma (Blanchard et al. 2011), showing that the AGE.HN cell line is an alternative and favorable expression system for the large-scale production of recombinant human A1AT.

The final product titer in a therapeutic protein production process in cell culture is related to high viable cell density and culture longevity (Kumar et al. 2007). In order to obtain high cell densities in a targeted development process, detailed knowledge of the metabolism of the producing cell system is desirable (Niklas et al. 2010). Metabolism of cells can be analyzed by metabolic profiling where, e.g., time courses of metabolites are interpreted or by different methods of metabolic flux analysis where intracellular reaction rates are analyzed (Niklas and Heinzle 2011; Niklas et al. 2010). Analysis of the cellular fluxome has shed light on the metabolism and its regulation not only in several mammalian cells (Bonarius et al. 2001; Gambhir et al. 2003; Niklas et al. 2009, 2011b; Sidorenko et al. 2008; Teixeira et al. 2008) but also in microorganisms (Selvarasu et al. 2009; Wittmann and Heinzle 2002) or plants (Heinzle et al. 2007).

In a metabolic flux study on parental AGE1.HN cells, changes in the metabolic fluxes during batch cultivation of the parental AGE1.HN cell line were analyzed (Niklas et al. 2011b). It was found that during cultivation, the metabolism in AGE1.HN was switching from an inefficient metabolic state characterized by waste product formation to a very efficient metabolic state with minimum energy spilling. The main event that was triggering this change in the metabolism was concluded to be the reduction in extracellular substrate levels including the depletion of pyruvate. Reduction of the glutamine level and finally its depletion was another perturbation occurring during batch cultivation, which led again not only to a metabolic shift but also to a stop of growth and reduction of viability. It seems interesting to investigate the effects of pyruvate and glutamine on growth, metabolism, and glycoprotein production in more detail. Especially, pyruvate was often not considered and sometimes even not measured in metabolic studies on mammalian cells. However, it was shown that pyruvate can be used to introduce beneficial changes in the metabolism of several mammalian production cells (Genzel et al. 2005; Omasa et al. 2009). Genzel et al. (2005) showed that high pyruvate concentrations in the medium can be used to replace glutamine, resulting in similar growth and lower ammonia production in cultivations of MDCK, BHK21, and CHO-K1 cells. These mammalian cells could even grow in media containing up to 37 mM pyruvate. Omasa et al. (2009) found that the addition of pyruvate to cultivations of CHO cells resulted in an increased tricarboxylic acid (TCA) cycle activity accompanied by increased ATP and antibody production rates. The mentioned studies show that it is interesting to investigate the effects of different substrate levels and especially different pyruvate concentrations on the metabolism to acquire an improved understanding of the cellular utilization of the substrates and their influence on cell growth and productivity. This improved understanding can eventually lead to the identification of promising targets for further metabolic engineering and rational improvement of the production process.

Aiming at understanding the influence of major substrates on the metabolism and growth of AGE1.HN, different substrate levels were examined. The effects of start concentrations of pyruvate and glutamine on the growth and metabolism of AGE1.HN in batch cultivation were studied using a full factorial design experiment. Based on these results, feeding experiments were carried out in which glucose, pyruvate, and glutamine were fed during the cultivation to maintain the substrate levels in a certain concentration range. Metabolic flux analysis using the metabolite balancing method was additionally performed for the differently fed cultures to analyze the differences in substrate use. The results of the study lead directly to further engineering strategies for the improvement of biopharmaceutical production in the human AGE1.HN cell line.

Material and methods

Cell lines and cell culture

The AGE1.HN® cell line (ProBioGen AG, Berlin, Germany) was developed from primary cells from a human

brain tissue sample. A more detailed description of the cell line was published recently (Niklas et al. 2011b). In this study, the parental AGE1.HN cell line as well as a derived production cell line (AGE1.HN.AAT) which is producing the therapeutic protein A1AT were applied. Parental AGE1.HN cells were transfected with an expression vector containing the human A1AT gene driven by a human CMV/EF1 hybrid promoter (ProBioGen AG). The high producing AGE1.HN.AAT cell line was derived after selection with puromycin. AGE1.HN cells were cultivated in the serum-free 42-Max-UB medium (Teutocell AG, Bielefeld, Germany). T-CHO ATIII cells producing recombinant anti-thrombin III were obtained from the Helmholtz Center for Infection Research (Braunschweig, Germany) and were cultured using serum-free CHO-S-SFM II medium (GIBCO, Invitrogen, Darmstadt, Germany). Standard cultivations of all cell lines were carried out in shake flasks (125 or 250 ml; Corning, NY, USA) at 37°C in an incubator containing a shaking unit (Innova 4230, New Brunswick Scientific, Edison, NJ, USA, 2-in. orbit) with constant 5% CO_2 supply at 185 rpm.

Analytical methods

Cell counting was performed using an automated cell counter (Countess, Invitrogen, Karlsruhe, Germany) or a hemocytometer. Viability was assessed applying the Trypan blue exclusion method. The pH in the samples was determined using a MP 220 pH meter (Mettler-Toledo, Giessen, Germany). Sugars, lactate, and pyruvate in the supernatant were analyzed using high-pressure liquid chromatography (HPLC) as described previously (Niklas et al. 2009). For the feeding experiments, glucose concentration was additionally measured using the Glucose-UV Assay Kit (Roche, Darmstadt, Germany) according to the manual. Quantification of proteinogenic amino acids was performed by HPLC using the method of Kromer et al. (2005). Ammonia was quantified using the ammonia assay kit of Sigma-Aldrich (Steinheim, Germany) according to the kit's instructions. The measurement was performed in a photometer (Novaspec, Pharmacia Biotech, LittleChalfont, England). The concentration of active A1AT was determined using the trypsin inhibitory assay. Calibration was done using standards with different A1AT concentrations (0.5–0.001 mg/ml in phosphate-buffered saline (PBS); A1AT from human plasma was acquired from Sigma-Aldrich). The samples were diluted with PBS (1:20 to 1:60). Of the samples and standard solutions, 50 μl was mixed with a trypsin solution (0.1 mg/ml in an activity buffer containing 15 mM Tris, 100 mM NaCl, 0.01% (*v*/*v*) Triton X-100 at pH 7.6) and incubated for 10 min at 37°C. Of these solutions, 10 μl was pipetted into the wells of a 96-well plate and 90 μl of a BAPNA solution (Nα-benzoyl-L-arginine 4-nitroanilide hydrochloride, Sigma-Aldrich) was added to each well. The BAPNA solution was prepared by mixing 11 μl of BAPNA stock solution (500 mM in DMSO) with 1,989 μl activity buffer. The plate was incubated at 37°C for 1 h and the absorption finally measured at 405 nm (iEMS Reader MF, Labsystems, Helsinki, Finland).

Study of the effects of pyruvate and glutamine concentrations

The effects of pyruvate and glutamine on the metabolism of the parental AGE1.HN cells were analyzed in a three-level full factorial design for both factors (glutamine and pyruvate), resulting in 3^2 cultivations. The applied pyruvate concentrations were 2, 5, and 9 mM; the glutamine concentrations were 5, 7.5, and 10 mM. The preculture was performed in normal 42-Max-UB medium (2 mM pyruvate, 5 mM glutamine). The cells were harvested by centrifugation (500 rpm, 5 min, 25°C; Labofuge 400R Function Line, Heraeus Instruments, Hanau, Germany) and the supernatant discarded. The cell pellet was resuspended in the medium without glutamine and pyruvate. The cell suspension was uniformly distributed into 50-ml bioreactor filter tubes (TPP, Trasadingen, Switzerland) and the supplements (glutamine, pyruvate) were added. The culture volume was 20 ml. Samples of 300 μl were taken every day. Of the samples, 50 μl was used directly for cell counting. The rest was centrifuged (8,000 rpm, 5 min, 25°C; Biofuge Pico, Heraeus Instruments), the supernatant transferred into fresh tubes, and frozen (−20°C) for later exometabolome analysis.

Cultivation of AGE1.HN.AAT using different substrate feeding

The effects of different feeding profiles of glucose and pyruvate on growth, metabolism, and product formation (A1AT) were analyzed. The preculture (42-Max-UB medium; 2 mM pyruvate, 2 mM glutamine) was harvested by centrifugation (500 rpm, 5 min, 25°C; Labofuge 400R Function Line, Heraeus Instruments) and the supernatant discarded. The pellets were washed once with PBS (37°C, centrifugation as before) and the cells were finally resuspended in 42-Max-UB medium without glucose and glutamine. After cell counting, the cell suspension was transferred into 50-ml bioreactor filter tubes (TPP) and the supplements were added. Glutamine (stock solution 200 mM) was added to a final concentration of 2 mM in all cultures and glucose (stock solution 200 g/l) was supplemented such that the concentration was 1 g/l (feeds 1 and 2) or 2 g/l (feeds 3 and 4). The total cultivation volume was 16 ml. The following cultivations were carried out: (1) control (batch), normal batch cultivation using the

standard cultivation conditions; (2) feed 1 (high Glc), glucose controlled at a high level (up to 2 g/l and mostly above 0.2 g/l); (3) feed 2 (high Glc + Pyr), glucose controlled at a high level (up to 2 g/l and mostly above 0.2 g/l) and when glucose was fed pyruvate was added such that the pyruvate concentration in the medium was increased by about 2 mM; (4) feed 3 (low Glc), glucose controlled at a low level (up to 1 g/l and mostly above 0.1 g/l); (5) feed 4 (low Glc + Pyr), glucose controlled at a low level (up to 1 g/l and mostly above 0.1 g/l) and when glucose was fed pyruvate was added such that the pyruvate concentration in the medium was increased by about 1 mM. In all cultivations, glutamine was fed to avoid limitation. Samples for metabolite analysis were taken every day. Glucose was measured in the cultures more often to avoid any limitation and to maintain the planned feeding profile by adjusting the feeding amount.

Metabolic flux analysis

Metabolic fluxes in AGE1.HN upon different substrate feeding were calculated for the phase between 72 and 169 h in which the main differences in the metabolism were observed. Stationary metabolic flux analysis was applied as described in detail in a recent publication (Niklas et al. 2011b). The metabolic network that was used recently to analyze metabolic shifts in the parental AGE1.HN cell line (Niklas et al. 2011b) was slightly modified and extended such that it contains additionally the production of A1AT and its precursor demand. The amino acid demand for A1AT was derived directly from its amino acid sequence. The average glycosylation of A1AT was taken from the literature (Kolarich et al. 2006). To glycosylate one A1AT protein having three *N*-glycosylation sites, the following sugar combination is needed: average glycosylation (three sites)=12.69 *N*-acetylglucosamine + 9 mannose+6.69 galactose + 6.681 *N*-acetylneuraminic acid + 0.321 fucose. The stoichiometry to synthesize 1 mol of fully glycosylated and active A1AT was included into the metabolic network model and can be seen in the stoichiometric matrix which is presented in Electronic supplementary material (ESM) Table S1. A scheme of the applied metabolic network is depicted in Fig. 1.

Enzyme assays

Enzyme activity measurements were carried out in cuvettes using a UV/vis photometer (Helios α, Spectronic Unicam, Cambridge, England) set at 37°C. For performing enzyme assays, 50 µl of cell suspension (10 µl for lactate dehydrogenase (LDH) assay) was pipetted in each cuvette and 950 µl of the respective assay solution (37°C) was added (990 µl for LDH assay). Chemicals (analytical grade) were purchased from Sigma-Aldrich, Fluka (Buchs, Switzerland), and Merck (Darmstadt, Germany). PBS buffer was acquired from PAA Laboratories (Pasching, Austria). The assay solutions for different enzymes were as follows. *Malic enzyme* (ME): 890 µl PBS, 10 µl $MgCl_2$ (200 mM), 10 µl $NADP^+$ (100 mM), and 40 µl malate (1 M). *LDH*: 960 µl PBS, 25 µl NADH (15 mM), and 5 µl pyruvate (500 mM). *Pyruvate carboxylase* (PC): 830 µl PBS, 10 µl $MgCl_2$ (1 M), 15 µl acetyl coenzyme A (50 mM), 10 µl $KHCO_3$ (1 M), 40 µl 5,5′-dithio-bis-(2-nitrobenzoic acid) (DTNB, 5 mM), 20 µl pyruvate (2 M), 25 µl ATP (100 mM), and 0.3 U citrate synthase. *Phosphoenolpyruvate carboxykinase* (PEPCK): 834 µl PBS, 15 µl NADH (10 mM) 1 µl $MgCl_2$ (1 M), 10 µl phosphoenolpyruvate (100 mM), 75 µl inosine diphosphate (20 mM), 10 µl malate dehydrogenase (>12 U), and 5 µl $KHCO_3$ (1 M). The cells were harvested in the exponential growth phase by centrifugation (5 min, 500 rpm, 25°C; Labofuge 400R, Heraeus Instruments). The supernatant was discarded and the pellet resuspended in PBS (37°C). This washing step was repeated and finally the pellet was resuspended in PBS and the cell density determined. The cell suspension was diluted to yield a cell density of ~5×10^6 cells/ml. The cells were disrupted by adding a Triton X-100 solution (5%, *v*/*v*) such that the final concentration in the cell suspension was 0.05% (*v*/*v*) followed by incubation at 37°C for 10 min. This treatment was earlier found sufficient to permeabilize cellular and mitochondrial membranes (Niklas et al. 2011a). The cells were transferred into the cuvettes and the enzyme assay solution was added. The change in absorbance was finally monitored for 15 min. The specific enzyme activities per cell (SA) were calculated using

$$\mathrm{SA} = \frac{\Delta A}{\Delta t \times \varepsilon \times \mathrm{CD}} \quad (1)$$

where A represents absorbance, CD the respective cell density, and t is time. For NAD(P)H-dependent measurements, the extinction coefficient, ε_{340}, of 6.22 $\mathrm{l\,mmol^{-1}\,cm^{-1}}$ was used; for the DTNB-dependent measurements, the extinction coefficient, ε_{412}, of 13.6 $\mathrm{l\,mmol^{-1}\,cm^{-1}}$.

Results

Growth and metabolic profiles at different initial pyruvate and glutamine concentrations

AGE1.HN cells were grown in batch culture using media with different pyruvate (Pyr) and glutamine (Gln) concentrations in a full factorial design experiment to analyze the effects of both metabolites on growth and metabolism. Changes in cell density and in selected metabolite concentrations during cultivation are shown in the surface plots in Fig. 2 and in ESM Table S2. The growth and metabolic

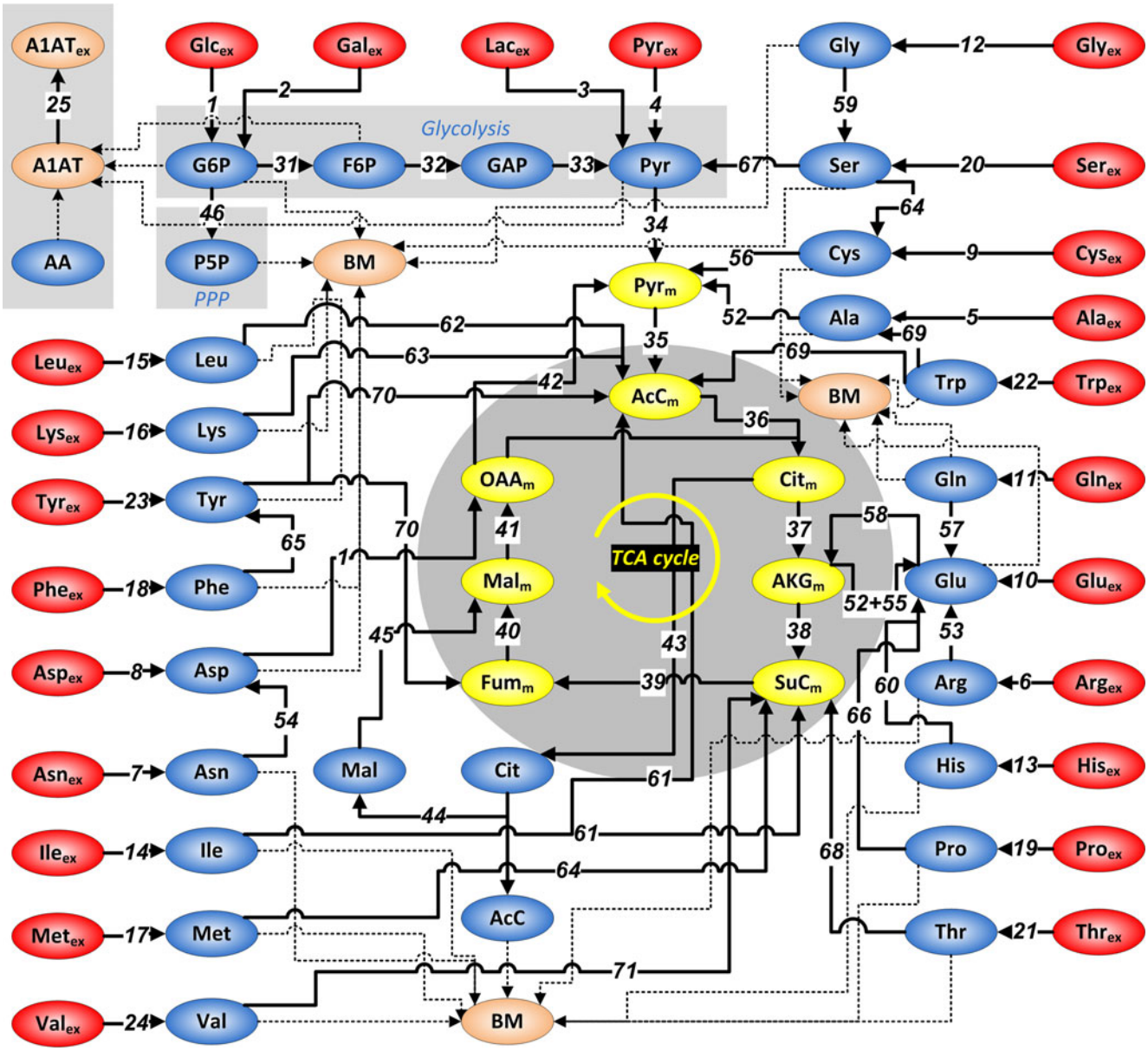

Fig. 1 Simplified scheme of the metabolic network model for the calculation of metabolic fluxes in AGE1.HN (modified and extended versions of a metabolic network model which was published previously; Niklas et al. 2011b). *Dotted lines* indicate fluxes to biomass (*BM*); *solid lines*, extracellular or intracellular fluxes. Flux numbers are depicted for extracellular and intracellular reactions. The stoichiometric matrix of the model is given in ESM Table S1. *PPP* pentose phosphate pathway, *TCA* tricarboxylic acid, *BM* biomass, *AA* all amino acids, *A1AT* α_1-antitrypsin, *Glc* glucose, *Gal* galactose, *Lac* lactate, *Pyr* pyruvate, *G6P* glucose 6-phosphate, *P5P* pentose 5-phosphate, *F6P* fructose 6-phosphate, *GAP* glyceraldehyde 3-phosphate, *AcC* acetyl coenzyme A, *Cit* citrate, *AKG* α-ketoglutarate, *SuC* succinyl coenzyme A, *Fum* fumarate, *Mal* malate, *OAA* oxaloacetate (standard abbreviations for amino acids). Indices: *m* mitochondrial, *ex* extracellular

profiles of all nine cultivations are depicted in ESM Fig. S1. Increasing Pyr concentrations led to a decrease in cell proliferation as well as total glucose, glutamine, and uptake of most amino acids (Fig. 2). Pyruvate uptake was highest in media having 5 mM Pyr as start concentration and was similar at high (9 mM) and low (2 mM) Pyr in the medium. Total lactate production was also highest in the 5 mM Pyr cultivations, but only slightly lower in the cultivations with 9 and 2 mM Pyr. The lactate/glucose quotient (ΔLac/ΔGlc) that is also depicted in Fig. 2 as well as the quotient of C-mol of produced lactate per C-mol of the consumed substrates glucose and pyruvate (CLac/(CGlc + CPyr)) indicate clearly a Pyr-dependent increase in the relative lactate production per consumed substrates. In the 9 mM Pyr cultivations, a CLac/(CGlc + CPyr) quotient of even around 1 was observed. Additionally, glutamate and alanine production was influenced by an increasing Pyr concentration. An increase in the Gln concentration does not influence the cell

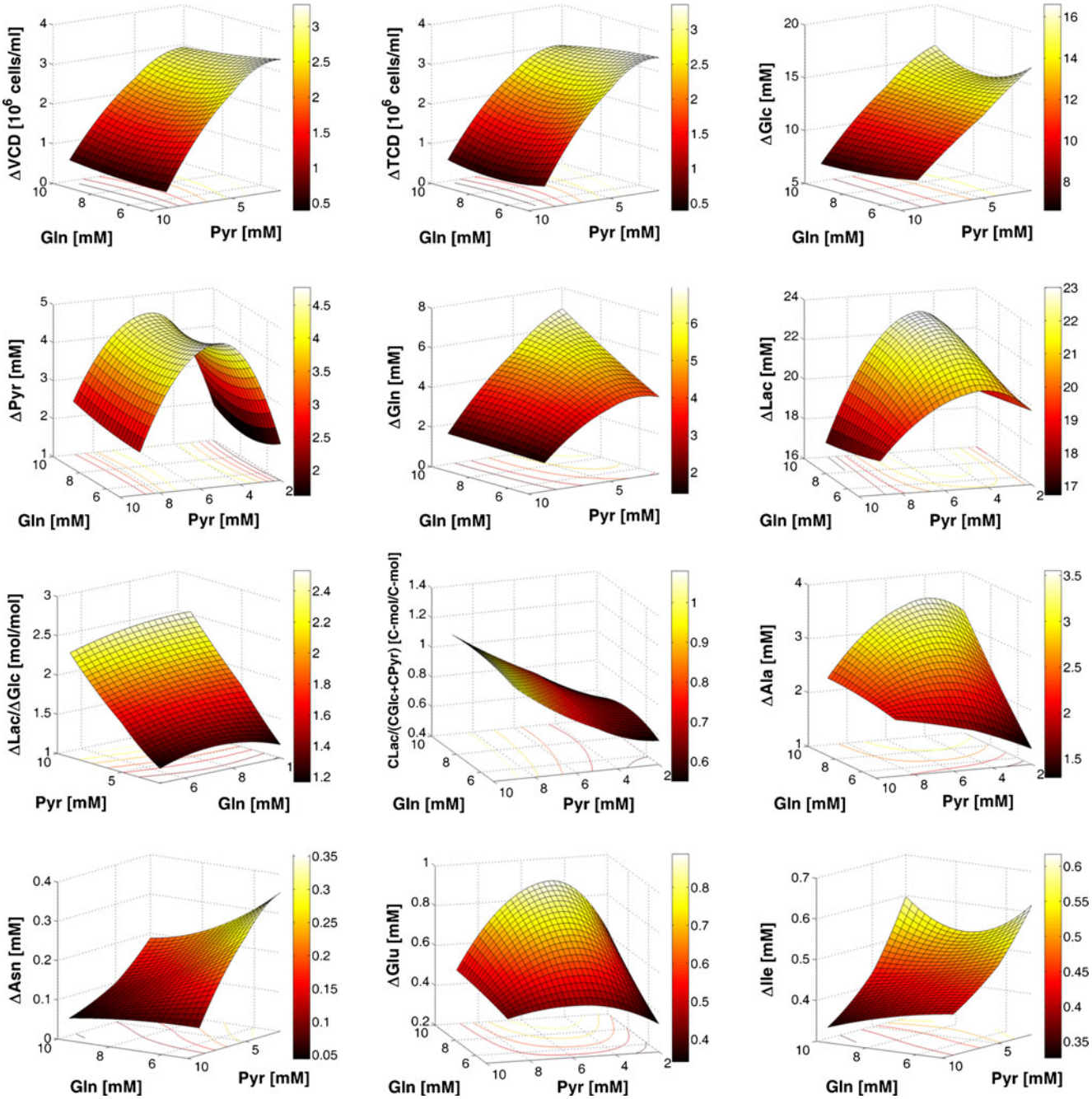

Fig. 2 Effects of different pyruvate (*Pyr*) and glutamine (*Gln*) concentrations in the medium on growth and extracellular metabolite levels (M) in AGE1.HN. Maximum changes, ΔM = |Maximum (M) − Minimum (M)|, in viable and total cell density (VCD, TCD) and extracellular metabolite levels (*Glc* glucose, *Lac* lactate (standard abbreviations for amino acids)) are depicted. Additionally, the total Lac/Glc quotient (ΔLac/ΔGlc) and the quotient of C-mol of produced lactate per C-mol of consumed glucose and pyruvate (CLac/(CGlc + CPyr)) in the different cultivations are presented. Detailed data are additionally given in ESM Table S2. Growth and metabolic profiles are depicted in ESM Fig. S1

proliferation, but led to an increase in the production of alanine, glutamate, and ammonia as well as a decrease in the uptake of asparagine and the branched chain amino acid isoleucine (Fig. 2 and ESM Table S2). Changes in extracellular metabolite concentrations per cell in the respective culture are depicted for some selected metabolites in Fig. 3. The data indicate that glucose and pyruvate uptake as well as the production of lactate per cell were increased depending on Pyr and only little influenced by changing Gln concentration. Alanine and glutamate production as well as glutamine uptake per cell were increased with increasing Gln and Pyr consumption.

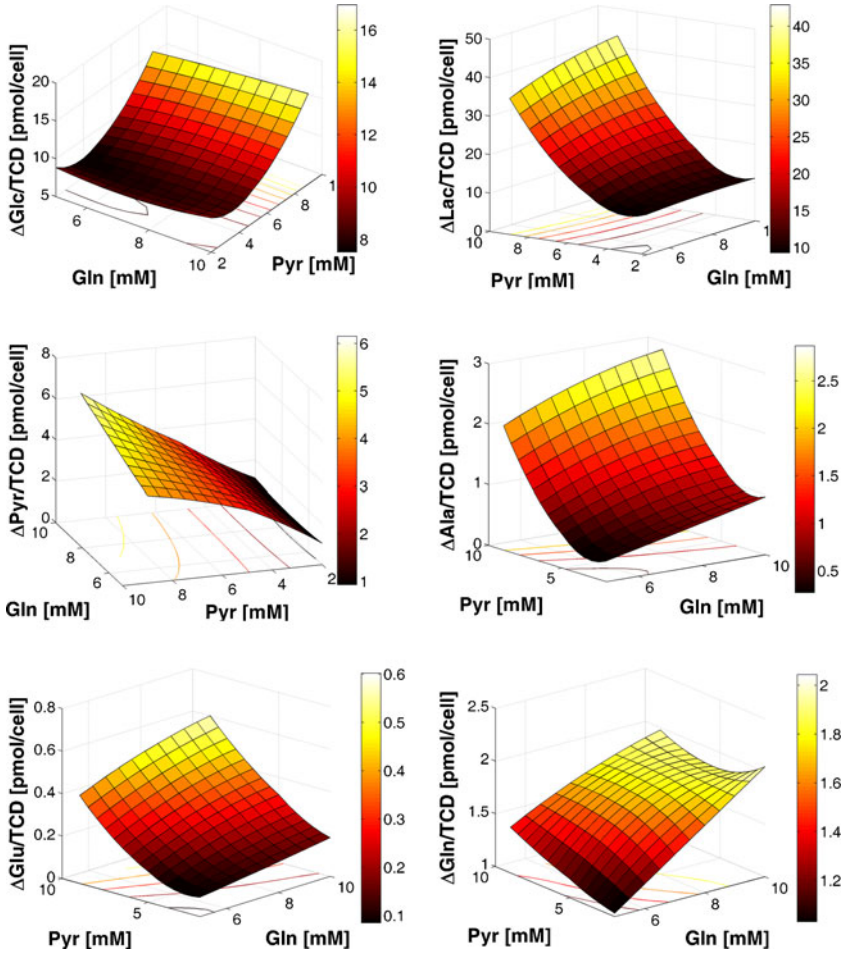

Fig. 3 Effects of different pyruvate (*Pyr*) and glutamine (*Gln*) concentrations in the medium on the metabolite uptake or production per total cell density (*TCD*). Maximum changes, Δ*M*, in extracellular metabolite levels per total cell density in each cultivation are depicted (*Glc* glucose, *Lac* lactate (standard abbreviations for amino acids)). Growth and metabolic profiles are depicted in ESM Fig. S1

Effects of different substrate feeding on growth and A1AT production

In the experiments described before with different pyruvate and glutamine concentrations, one of the most interesting aspects was the fact that increasing pyruvate concentrations led to low growth performance and high energy spilling, as indicated by high waste product formation. This effect of higher substrate load leading to energy wasting was further investigated by applying different feeding profiles. For these experiments, AGE1.HN cells producing the therapeutic glycoprotein A1AT were used to additionally get insights into the product formation under varying conditions of substrate supply. Different substrate feeding rates and different substrate concentrations in the medium might result in a different intracellular pyruvate supply and further changes in the cellular metabolism and product formation. The applied feeding profiles are depicted in Fig. 4. Different supplies of glucose and pyruvate were tested in the four feeding experiments. Growth and metabolite profiles (only the most important metabolites) are depicted in Fig. 5. In the beginning, growth and metabolism were similar in the fed-batch cultures and the batch cultivation. In a second phase after 72 h of cultivation, metabolism was clearly different depending on the applied feeding profile. The lower initial glucose concentration combined with feeding resulted always in higher cell density, increased culture longevity, and higher A1AT concentration compared with the batch cultivation. The highest viable cell density (146% of the batch cultivation) was achieved in the low-glucose culture without pyruvate feeding (Feed 3), in which also the highest A1AT concentration (167% of batch cultivation) was measured (Fig. 5). In the cultures that were also fed with pyruvate (feeds 2 and 4), lactate production was slightly higher after 72 h. Alanine and glutamate production were clearly increased compared with the cultures without the addition of pyruvate. Furthermore, A1AT production was lower in the cultures which were additionally fed with pyruvate.

Metabolic changes upon different substrate feeding

In order to understand the main metabolic differences caused by different feeding of the substrates, glucose and

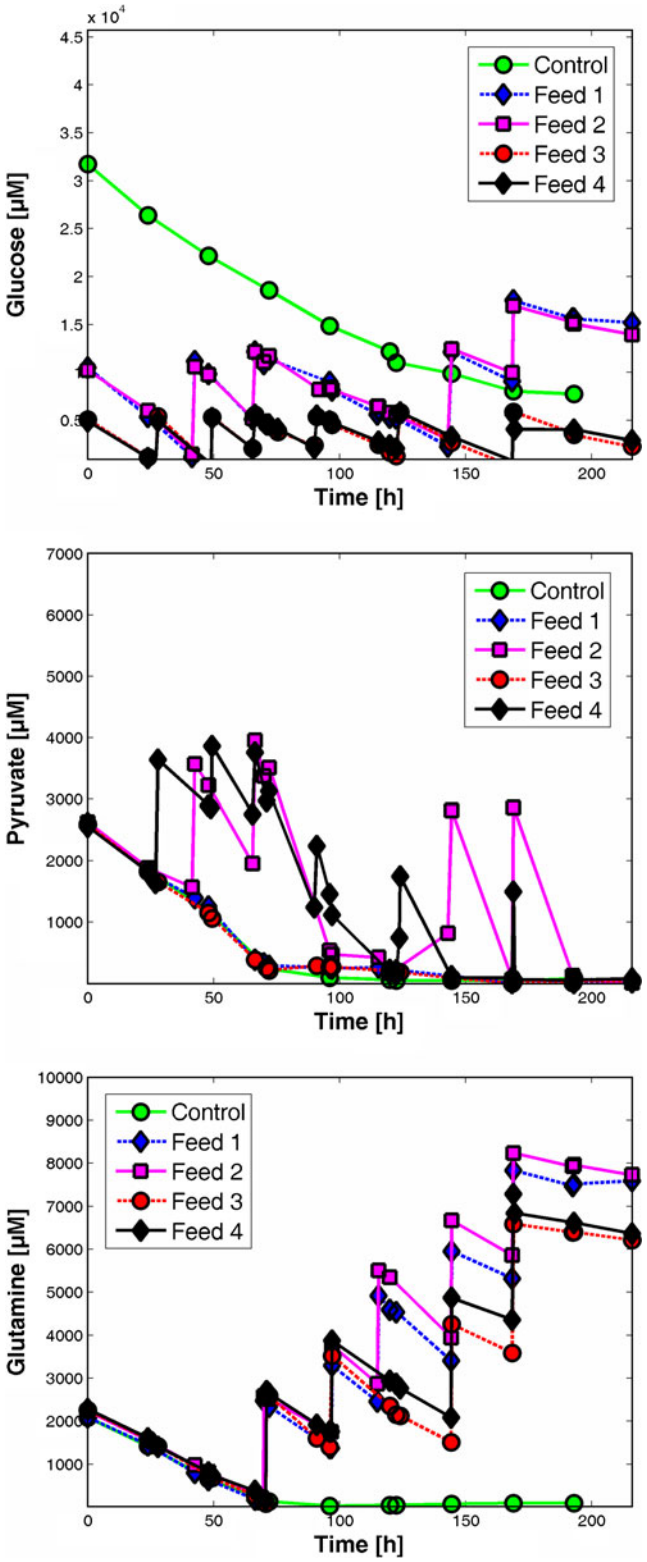

Fig. 4 Profiles of glucose (*Glc*), glutamine (*Gln*), and pyruvate (*Pyr*) concentrations during cultivations of the AGE1.HN.AAT cell line with different feeding profiles. Control (batch), normal batch cultivation using standard cultivation conditions; feed 1 (high Glc), glucose controlled at a high level (up to 2 g/l and mostly above 0.2 g/l); feed 2 (high Glc + Pyr), glucose controlled at a high level (up to 2 g/l and mostly above 0.2 g/l). When glucose was fed, pyruvate was added such that the pyruvate concentration in the medium was increased by about 2 mM; feed 3 (low Glc), glucose controlled at a low level (up to 1 g/l and mostly above 0.1 g/l); feed 4 (low Glc + Pyr), glucose controlled at a low level (up to 1 g/l and mostly above 0.1 g/l). When glucose was fed, pyruvate was added such that the pyruvate concentration in the medium was increased by about 1 mM. Glutamine was additionally fed to avoid limitation

pyruvate stationary metabolic flux analysis was performed for the phase between 72 and 169 h of the cultivation (Fig. 6 and ESM Table S3) in which the main differences in metabolite and growth profiles were observed (Fig. 5 and ESM Fig. S2). It was found that the glucose uptake rate and glycolytic fluxes (v_{32}, Fig. 6) were only slightly reduced when pyruvate was fed as an additional carbon source (feed 2 and feed 4). Lactate production rate (v_3, Fig. 6) was clearly increased in the cultures with pyruvate feeding. Mitochondrial pyruvate transport seemed to be slightly reduced with pyruvate feeding and with a lower glucose concentration in the medium (v_{34}, Fig. 6). The activity of the upper and lower TCA cycle (v_{36} and v_{38}, Fig. 6) was unaffected by pyruvate feeding (feed 2 and feed 4), but was decreased in the cultures fed with low glucose levels (feed 3 and feed 4). The TCA cycle was mainly fed by pyruvate. Glutamate carbons were entering the TCA cycle to a lower extent and solely through transaminase-catalyzed conversion ($v_{52} + v_{55}$, Fig. 6). Glutamate dehydrogenase was working in the direction of glutamate (v_{58}, Fig. 6). This flux was clearly increased in the low-glucose cultures and slightly decreased when additionally pyruvate was fed. Net flux from glutamate to α-ketoglutarate ($v_{58} - (v_{52} + v_{55})$) was increased with pyruvate feeding (feed 2 and feed 4) and lower in the low-glucose cultures (feed 3 and feed 4) compared with the high-glucose cultures (feed 1 and feed 2). This flux was generally around 12% of the pyruvate transport flux (v_{34}). Glutamate and alanine production rates (v_5 and v_{10}, Fig. 6) were increased depending on pyruvate, as also observed for the lactate production rate. The highest A1AT production rate was found in the culture feed 3 in which glucose was maintained at a low level and pyruvate was not fed.

Comparative analysis of in vitro activities of selected anaplerotic enzymes

In vitro activities of important enzymes of the pyruvate metabolism were measured in parental (AGE1.HN Par) and A1AT-producing (AGE1.HN.AAT) AGE1.HN cells and compared with the corresponding enzyme activity in a CHO cell line (T-CHO ATIII cells producing recombinant anti-thrombin III; Table 1). ME activity was slightly lower, whereas PC and PEPCK activities in AGE1.HN were by far lower than in CHO. Lactate dehydrogenase activity was slightly higher in AGE1.HN cell lines compared with CHO cells.

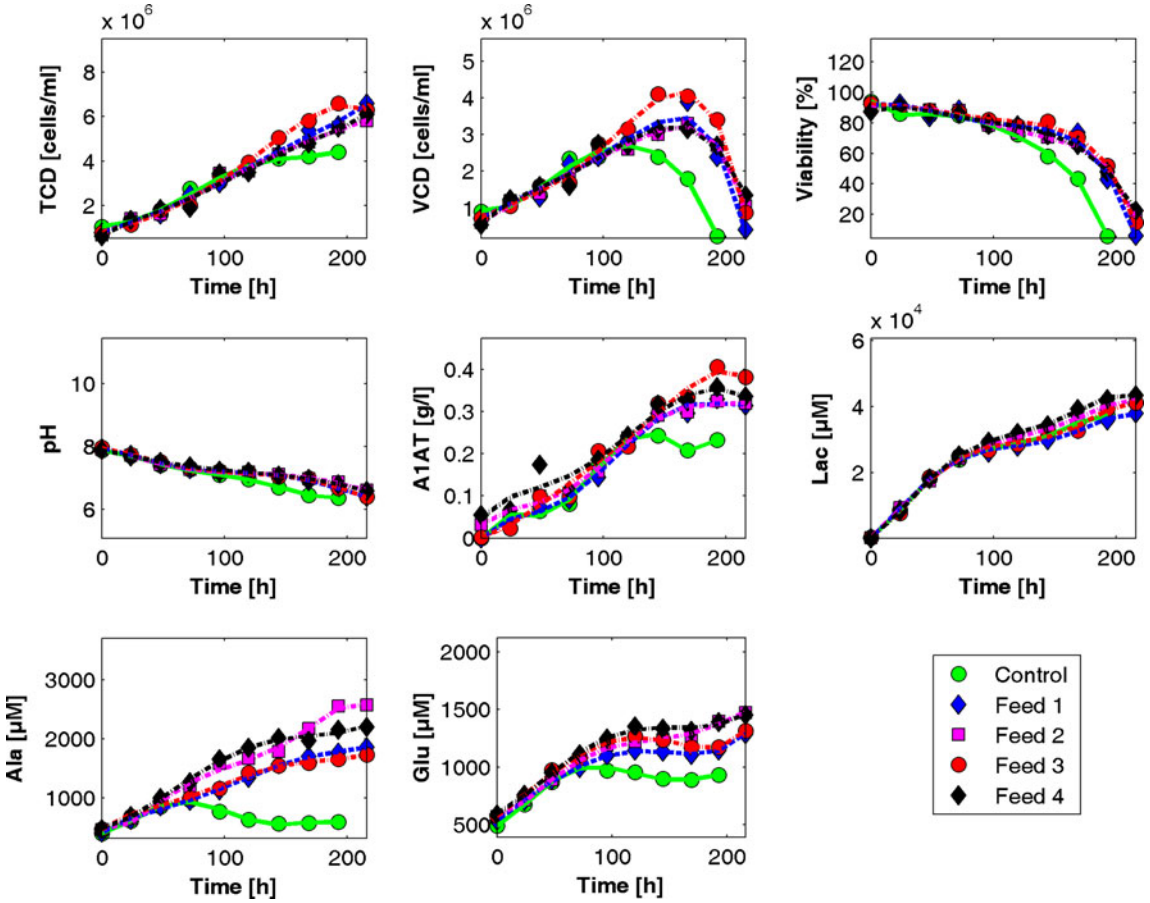

Fig. 5 Growth and metabolic profile of AGE1.HN.AAT cells during cultivation. The same experiment as in Fig. 4 where the applied feeding profiles are depicted. *TCD* total cell density, *VCD* viable cell density, *A1AT* α_1-antitrypsin, *Lac* lactate (standard abbreviations for amino acids)

Discussion

In the first part of this study, the growth and metabolic profiles of AGE1.HN cells cultured with increasing pyruvate and glutamine concentrations were analyzed. In a recent study on metabolic dynamics, it was proposed that pyruvate and glutamine supply might induce characteristic changes in the metabolism of AGE1.HN (Niklas et al. 2011b). This was based on flux changes analyzed during batch cultivation. In order to investigate the influence of both substrate metabolites in detail, increased pyruvate and glutamine concentrations were applied in a full factorial design experiment and the growth and metabolite concentrations were monitored. The dependency of the production and uptake of other metabolites on extracellular pyruvate and glutamine levels could be determined.

Increased glutamine concentrations did not cause significant changes in cell proliferation, but led to specific changes in the uptake and production of other amino acids and amino group donors as well as an increase in ammonia production (ESM Table S1). Increased alanine production caused by increased glutamine concentration in the medium aids in reducing ammonia intoxication. Transamination reactions, transferring amino groups from aspartate or glutamate to pyruvate, yielding alanine, may play a role in ammonia detoxification. Also in other studies, increased alanine production in the presence of high ammonia concentrations was reported (Hansen and Emborg 1994; Miller et al. 1988; Ozturk et al. 1992). In AGE1.HN, it was additionally found that glutamine depletion is associated with a direct decrease in viability, showing its importance for this cell line (Niklas et al. 2011b). After glutamine depletion, the metabolism tries to compensate this by a higher uptake of the amino group donors glutamate and alanine, but this is not enough to sustain the growth rate and viability (Niklas et al. 2011b). Glutamine feeding seems essential to maintain the viability and growth of AGE1.HN, as will also be outlined later in the discussion.

The cell interior of mammalian cells is compartmentalized and highly organized. To overcome diffusive barriers in the cell, enzymes of a metabolic pathway are sometimes associated physically and build static multienzyme complexes, so-called metabolons, resulting in a channeling of the metabolites through this pathway (Ovadi and Saks

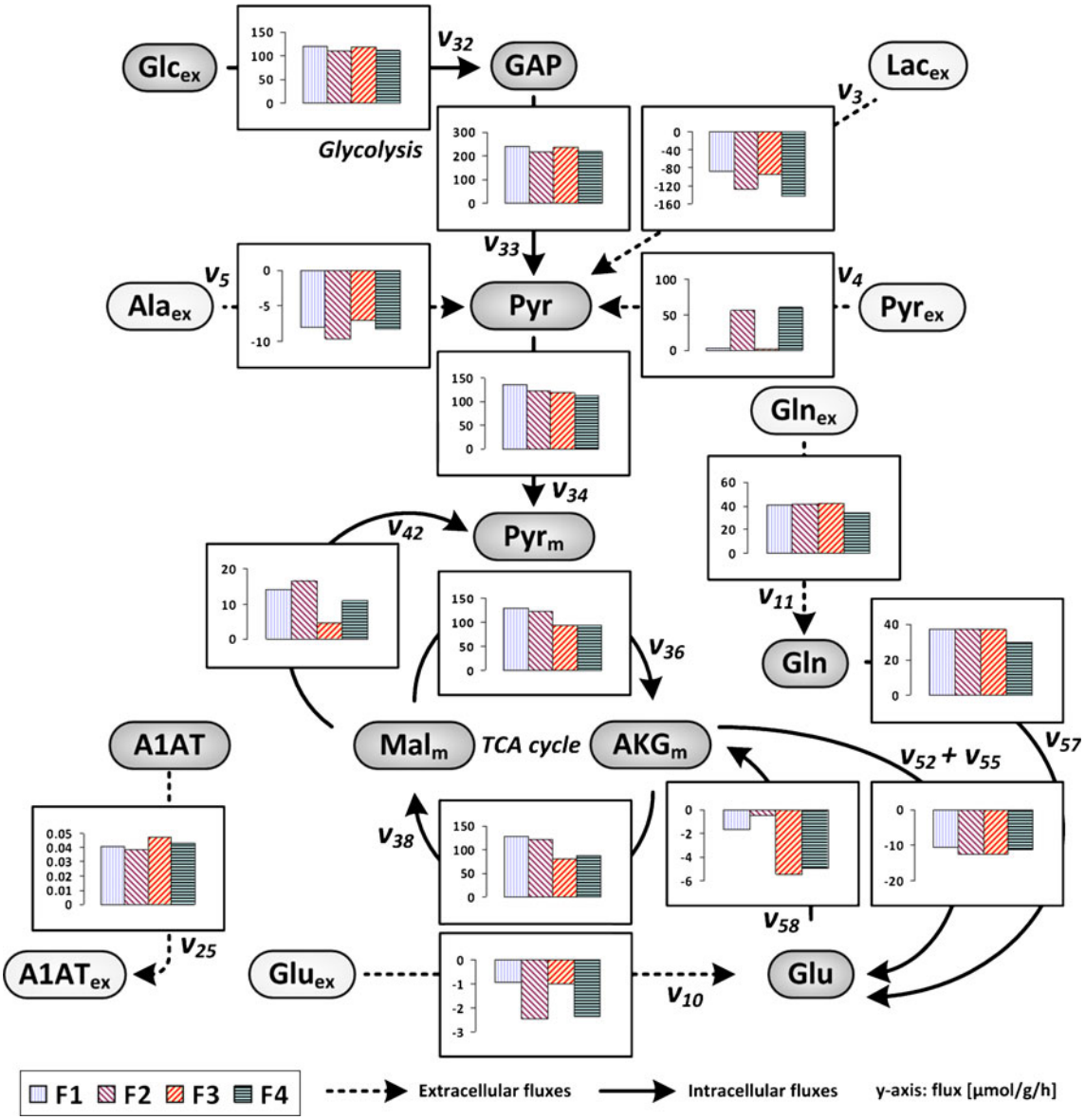

Fig. 6 Metabolic flux distribution of AGE1.HN during cultivations in which different feeding profiles (*F1–F4* correspond to feed 1–feed 4 of Fig. 4) were applied. The same experiment as shown in Figs. 4 and 5. Fluxes were calculated for the phase between 72 and 169 h. Negative values indicate fluxes in the opposite direction of the *arrow*. Detailed data are additionally presented in ESM Table S3. The metabolic network including the flux numbers of the reactions and the abbreviations can be seen in Fig. 1

2004). Glycolytic channeling and the association of glycolytic enzymes has been reported earlier (Graham et al. 2007). This might result in a direct conversion of glucose down to lactate, preventing an efficient use of glucose-derived pyruvate in the mitochondria. Additional cytoplasmic pyruvate pools could exist (Zwingmann et al.

Table 1 In vitro activities of the enzymes ME, PC, PEPCK, and LDH in parental (AGE1.HN Par) and A1AT-producing (AGE1.HN.AAT) AGE1.HN cells as well as in T-CHO ATIII cells

	ME	PC	PEPCK	LDH
AGE1.HN Par	81.5 ± 8.4	77.0 ± 9.4	2,582.9 ± 32.5	14,337.8 ± 510.4
AGE1.HN.AAT	97.7 ± 2.3	183.0 ± 15.9	2,676.7 ± 25.4	14,255.9 ± 403.0
T-CHO ATIII	143.3 ± 5.5	515.3 ± 20.8	7,143.5 ± 284.2	12,504.1 ± 337.6

Activities were measured in the exponential growth phase of the cells. Mean values and standard deviations of two measurements. Specific enzyme activities are given in femtomoles per cell per hour

2001), and this pyruvate might be transported more efficiently into mitochondria and might be further metabolized in oxidative decarboxylation and TCA cycle. Omasa et al. (2009) found that the ATP and antibody production rates of hybridoma cells could be increased by adding specific metabolites, i.e., pyruvate, malate, and citrate. Especially, pyruvate enrichment caused an improvement of the energy metabolism (e.g., increase in TCA cycle fluxes) and a significant increase in product formation. In AGE1.HN cells, it seems that pyruvate has an opposite effect since growth and energy metabolism became less efficient with increasing pyruvate supply in the medium. Especially, lactate production per consumed substrate (glucose and pyruvate) increased. This indicates that pyruvate taken up from the medium is not differently and not more efficiently used than pyruvate derived through glycolysis. The performance of AGE1.HN is not improved by using additional pyruvate in the medium. Increasing pyruvate concentrations led to a less efficient metabolic phenotype with increased production of the waste metabolites lactate, alanine, and glutamate. This influence of pyruvate on the waste metabolite production was also proposed in a dynamic analysis of the metabolism of this cell line (Niklas et al. 2011b). Interestingly, an increase in the pyruvate supply was directly accompanied by an increase in lactate production per substrate that was taken up, resulting in an almost complete conversion of the substrates to lactate when 9 mM pyruvate was used in the medium (Fig. 1). This might also explain the almost complete stop of proliferation at the highest pyruvate concentration. The cells were not proliferating but were metabolizing the substrates, almost not producing any biomass but just waste metabolites. This indicates clearly that a reduction in the pyruvate load is beneficial for the growth of AGE1.HN and most probably also for later recombinant protein production.

However, the pyruvate load and especially intracellular pyruvate load is dependent not only on the pyruvate concentration in the medium and its uptake but also on the cellular glucose uptake and the glucose amount which is metabolized through glycolysis. Generally, substrate level reduction seems beneficial to improve the efficiency of metabolism of AGE1.HN. Since pyruvate is efficiently taken up by the cells (Niklas et al. 2011b), the high pyruvate concentrations applied in this experiment (Fig. 1) mimic also the situation in which the cell has to cope with high intracellular pyruvate concentrations. It can be clearly seen in this study that the cells are not able to use the additional substrates efficiently by adapting their uptake or by increasing pyruvate flux into the TCA cycle, which could result in better growth. Increased channeling of pyruvate into the TCA cycle depends on the possibility to increase pyruvate transport, pyruvate dehydrogenase activity, anaplerotic reactions, and respiration activity. However, this does not seem possible since the growth performance of the cells was clearly decreasing with increased substrate availability.

Another interesting application of high pyruvate concentrations in the medium was published by Genzel et al. (2005). It was reported that the replacement of glutamine by high pyruvate concentrations (e.g., 10 mM) seems to be an interesting strategy to reduce ammonia formation for some mammalian cell lines. However, when we tried to culture the human cell line AGE1.HN in media without glutamine, the cells were not growing even when increased concentrations of pyruvate were supplied (data not shown). Cultivation of the cells in media in which glutamine was replaced by glutamate was also not successful (data not shown). This might be caused by the low or absent glutamine synthetase activity that was reported for other human cells (Bell et al. 1995; Street et al. 1993).

The strong influence of pyruvate on the energy spilling in AGE1.HN might also partly be explained by the lower activity of anaplerotic enzymes, e.g., malic enzyme, pyruvate carboxylase, and phosphoenolpyruvate carboxykinase compared with CHO cells (Table 1). As shown by Genzel et al. (2005), other mammalian cells (but not human cells) grow comparably well in media having low or high pyruvate concentrations, which might be explained by a higher enzymatic capacity to convert pyruvate and channel its carbons into the TCA cycle associated with a higher respiratory activity. In a following metabolic flux study on MDCK cells in normal medium or medium having high pyruvate concentration and no glutamine, it was proposed that most of the glucose consumed was excreted as lactate under high pyruvate conditions whereas pyruvate seemed to directly enter the TCA cycle (Sidorenko et al. 2008). This is also different compared with AGE1.HN. The results of the feeding experiment (Fig. 4) and especially the metabolite balancing flux analysis (Fig. 6) showed that additional pyruvate does not lead to an increase in TCA cycle fluxes and was not beneficial for A1AT production. As mentioned before, anaplerotic reactions connecting glycolysis and the TCA cycle, the pyruvate dehydrogenase activity, or respiratory capacity might be the bottleneck resulting in the observed phenotype. The low in vitro activities of the measured anaplerotic enzymes (Table 1) and the inefficient pyruvate use can be an indication that a genetic engineering strategy, as was applied in other mammalian cells, might be also interesting for the improvement of the AGE1.HN cell line, namely, the introduction of an additional pyruvate carboxylase gene (Elias et al. 2003; Irani et al. 1999). However, this will only lead to a significant improvement if oxidative phosphorylation is not the limiting step.

The results of this study led to another strategy. A reduction in the substrate load (decrease in glucose concentration and no pyruvate feeding) resulted in improved culture longevity, more efficient metabolism, and finally higher product con-

centration. Substrate feeding should be balanced in fed-batch processes of AGE1.HN to maintain a most efficient metabolism. However, according to the data of the feeding experiments in which waste product formation was also just partially reduced even at the lowest glucose feeding, strategies focusing on the inhibition/reduction of substrate uptake should be considered. This may lead to lower accumulation of toxic waste products, higher cell densities, and product concentrations in the cultivation. Some genetic engineering in the past on mammalian cells focused also on the reduction of excessive substrate uptake, leading to an improved metabolism in the modified cells (Altamirano et al. 2000; Wlaschin and Hu 2007). Based on the results of this contribution, we have worked out a targeted engineering strategy for this cell line which focuses on a more efficient substrate usage, and work is underway showing the influence of this strategy on glycoprotein production in AGE1.HN.

Regarding the general findings concerning primary metabolism in AGE1.HN, it can be concluded that certain aspects are similar compared with the metabolic behavior of other mammalian cells, e.g., overflow metabolism in the beginning of the cultivation with high waste product formation, whereas other important metabolic parameters are completely different. Especially, pyruvate utilization and pyruvate metabolism are different in AGE1.HN compared with, e.g., CHO or MDCK cells, as was outlined before in the discussion.

Differences in the metabolism and in the metabolic machinery of different production cell lines might also originate from their specific origin. Enzyme and transporter properties as well as metabolic requirements of the cells depend on the tissue from which they originate (Wang et al. 2010). The cells in these tissues have a certain enzyme expression, e.g., different glucose transporters (Elsas and Longo 1992; Thorens and Mueckler 2010) or different expression of glycolytic and gluconeogenic enzymes (Lawrence et al. 1986), which depends also on their nutritional environment present in the respective part of the body (Mather and Pollock 2011). Different substrate levels in different tissues and even parts of tissues (Mather and Pollock 2011) result in cells adapted to their environment fulfilling specific tasks (Gebhardt 1992). Cells derived from different tissues might have therefore different metabolic properties, and their enzyme expression as well as the ability to adapt the enzyme expression to varying situations might differ. However, one has to keep in mind that production cells are immortalized and their metabolic behavior changes compared with the tissue situation. Nevertheless, these changes might be constrained to a certain extent depending on the tissue type from which the cells originate, e.g., by epigenetic mechanisms.

In summary, the following conclusions can be drawn from the different experiments which were performed in this study. Pyruvate enrichment in the medium leads to an inefficient metabolism characterized by high energy spilling and lowered cell proliferation. Reduced substrate levels and no pyruvate feeding resulted in a higher efficiency of substrate use as well as higher viable cell densities and A1AT concentrations. Pyruvate addition does not increase TCA cycle fluxes in AGE1.HN, contrary to reports using other mammalian cells. Generally, pyruvate utilization in AGE1.HN cells as well as fluxes around the pyruvate node seem to be significantly different compared with the other mammalian cells currently employed in biopharmaceutical production. The in vitro activity of the measured anaplerotic enzymes in AGE1.HN is lower compared with CHO cells and can be an interesting genetic engineering target for the improvement of AGE1.HN since pyruvate is not efficiently entering the TCA cycle. However, the most promising strategy in our opinion is the engineering of the cells toward a more balanced substrate uptake. Work is underway showing the effects of this engineering strategy on the production in AGE1.HN cells. The findings of this study provide a rational basis for further targeted improvement of the cellular metabolism and the cultivation process conditions for production cells.

Acknowledgments This work has been financially supported by the BMBF project SysLogics–Systems biology of cell culture for biologics (FKZ 0315275A-F). We thank Armin Melnyk for performing enzyme assays, Michel Fritz for valuable support for the HPLC analysis, as well as Judith Wahrheit for fruitful discussions.

References

A1AT-Group (1998) Survival and FEV1 decline in individuals with severe deficiency of alpha1-antitrypsin. The Alpha-1-Antitrypsin Deficiency Registry Study Group. Am J Respir Crit Care Med 158(1):49–59

al-Rubeai M, Singh RP (1998) Apoptosis in cell culture. Curr Opin Biotechnol 9(2):152–156

Altamirano C, Paredes C, Cairo JJ, Godia F (2000) Improvement of CHO cell culture medium formulation: simultaneous substitution of glucose and glutamine. Biotechnol Prog 16(1):69–75

Arden N, Betenbaugh MJ (2006) Regulating apoptosis in mammalian cell cultures. Cytotechnology 50(1–3):77–92

Bell SL, Bebbington C, Scott MF, Wardell JN, Spier RE, Bushell ME, Sanders PG (1995) Genetic engineering of hybridoma glutamine metabolism. Enzyme Microb Technol 17(2):98–106

Blanchard V, Liu X, Eigel S, Kaup M, Rieck S, Janciauskiene S, Sandig V, Marx U, Walden P, Tauber R, Berger M (2011) *N*-glycosylation and biological activity of recombinant human alpha1-antitrypsin expressed in a novel human neuronal cell line. Biotechnol Bioeng 108:2118–2128

Bonarius HP, Ozemre A, Timmerarends B, Skrabal P, Tramper J, Schmid G, Heinzle E (2001) Metabolic-flux analysis of continuously cultured hybridoma cells using $^{13}CO_2$ mass spectrometry in combination with ^{13}C-lactate nuclear magnetic resonance spectroscopy and metabolite balancing. Biotechnol Bioeng 74(6):528–538

Carrell RW, Jeppsson JO, Vaughan L, Brennan SO, Owen MC, Boswell DR (1981) Human alpha 1-antitrypsin: carbohydrate attachment and sequence homology. FEBS Lett 135(2):301–303

Cruz HJ, Moreira JL, Carrondo MJ (1999) Metabolic shifts by nutrient manipulation in continuous cultures of BHK cells. Biotechnol Bioeng 66(2):104–113

Elias CB, Carpentier E, Durocher Y, Bisson L, Wagner R, Kamen A (2003) Improving glucose and glutamine metabolism of human HEK 293 and *Trichoplusia ni* insect cells engineered to express a cytosolic pyruvate carboxylase enzyme. Biotechnol Prog 19 (1):90–97

Elsas LJ, Longo N (1992) Glucose transporters. Annu Rev Med 43:377–393

Gambhir A, Korke R, Lee J, Fu PC, Europa A, Hu WS (2003) Analysis of cellular metabolism of hybridoma cells at distinct physiological states. J Biosci Bioeng 95(4):317–327

Gebhardt R (1992) Metabolic zonation of the liver: regulation and implications for liver function. Pharmacol Ther 53(3):275–354

Genzel Y, Ritter JB, Konig S, Alt R, Reichl U (2005) Substitution of glutamine by pyruvate to reduce ammonia formation and growth inhibition of mammalian cells. Biotechnol Prog 21 (1):58–69

Gildea TR, Shermock KM, Singer ME, Stoller JK (2003) Cost-effectiveness analysis of augmentation therapy for severe alpha1-antitrypsin deficiency. Am J Respir Crit Care Med 167(10):1387–1392

Graham JW, Williams TC, Morgan M, Fernie AR, Ratcliffe RG, Sweetlove LJ (2007) Glycolytic enzymes associate dynamically with mitochondria in response to respiratory demand and support substrate channeling. Plant Cell 19(11):3723–3738

Hansen HA, Emborg C (1994) Influence of ammonium on growth, metabolism, and productivity of a continuous suspension Chinese hamster ovary cell culture. Biotechnol Prog 10(1):121–124

Heinzle E, Matsuda F, Miyagawa H, Wakasa K, Nishioka T (2007) Estimation of metabolic fluxes, expression levels and metabolite dynamics of a secondary metabolic pathway in potato using label pulse-feeding experiments combined with kinetic network modelling and simulation. Plant J 50(1):176–187

Irani N, Wirth M, van Den Heuvel J, Wagner R (1999) Improvement of the primary metabolism of cell cultures by introducing a new cytoplasmic pyruvate carboxylase reaction. Biotechnol Bioeng 66(4):238–246

Karnaukhova E, Ophir Y, Golding B (2006) Recombinant human alpha-1 proteinase inhibitor: towards therapeutic use. Amino Acids 30(4):317–332

Kelly E, Greene CM, Carroll TP, McElvaney NG, O'Neill SJ (2010) Alpha-1 antitrypsin deficiency. Respir Med 104(6):763–772

Kolarich D, Weber A, Turecek PL, Schwarz HP, Altmann F (2006) Comprehensive glyco-proteomic analysis of human alpha1-antitrypsin and its charge isoforms. Proteomics 6(11):3369–3380

Korke R, Gatti Mde L, Lau AL, Lim JW, Seow TK, Chung MC, Hu WS (2004) Large scale gene expression profiling of metabolic shift of mammalian cells in culture. J Biotechnol 107(1):1–17

Kromer JO, Fritz M, Heinzle E, Wittmann C (2005) In vivo quantification of intracellular amino acids and intermediates of the methionine pathway in *Corynebacterium glutamicum*. Anal Biochem 340(1):171–173

Kumar N, Gammell P, Clynes M (2007) Proliferation control strategies to improve productivity and survival during CHO based production culture: a summary of recent methods employed and the effects of proliferation control in product secreting CHO cell lines. Cytotechnology 53(1–3):33–46

Lawrence GM, Jepson MA, Trayer IP, Walker DG (1986) The compartmentation of glycolytic and gluconeogenic enzymes in rat kidney and liver and its significance to renal and hepatic metabolism. Histochem J 18(1):45–53

Mather A, Pollock C (2011) Glucose handling by the kidney. Kidney Int Suppl 120:S1–S6

Miller WM, Wilke CR, Blanch HW (1988) Transient responses of hybridoma cells to lactate and ammonia pulse and step changes in continuous culture. Bioprocess Eng 3(3):113–122, 113–122

Niklas J, Heinzle E (2011) Metabolic flux analysis in systems biology of mammalian cells. Adv Biochem Eng Biotechnol. doi:10.1007/10_2011_99

Niklas J, Noor F, Heinzle E (2009) Effects of drugs in subtoxic concentrations on the metabolic fluxes in human hepatoma cell line Hep G2. Toxicol Appl Pharmacol 240(3):327–336

Niklas J, Schneider K, Heinzle E (2010) Metabolic flux analysis in eukaryotes. Curr Opin Biotechnol 21(1):63–69

Niklas J, Melnyk A, Yuan Y, Heinzle E (2011a) Selective permeabilization for the high-throughput measurement of compartmented enzyme activities in mammalian cells. Anal Biochem 416(2):218–227

Niklas J, Schrader E, Sandig V, Noll T, Heinzle E (2011b) Quantitative characterization of metabolism and metabolic shifts during growth of the new human cell line AGE1.HN using time resolved metabolic flux analysis. Bioprocess Biosyst Eng 34(5):533–545

Nivitchanyong T, Martinez A, Ishaque A, Murphy JE, Konstantinov K, Betenbaugh MJ, Thrift J (2007) Anti-apoptotic genes Aven and E1B-19K enhance performance of BHK cells engineered to express recombinant factor VIII in batch and low perfusion cell culture. Biotechnol Bioeng 98(4):825–841

O'Callaghan PM, James DC (2008) Systems biotechnology of mammalian cell factories. Brief Funct Genomic Proteomic 7 (2):95–110

Omasa T, Takami T, Ohya T, Kiyama E, Hayashi T, Nishii H, Miki H, Kobayashi K, Honda K, Ohtake H (2008) Overexpression of GADD34 enhances production of recombinant human antithrombin III in Chinese hamster ovary cells. J Biosci Bioeng 106 (6):568–573

Omasa T, Furuichi K, Iemura T, Katakura Y, Kishimoto M, Suga K (2009) Enhanced antibody production following intermediate addition based on flux analysis in mammalian cell continuous culture. Bioprocess Biosyst Eng 33(1):117–125

Ovadi J, Saks V (2004) On the origin of intracellular compartmentation and organized metabolic systems. Mol Cell Biochem 256–257(1–2):5–12

Ozturk SS, Riley MR, Palsson BO (1992) Effects of ammonia and lactate on hybridoma growth, metabolism, and antibody production. Biotechnol Bioeng 39(4):418–431

Petrache I, Hajjar J, Campos M (2009) Safety and efficacy of alpha-1-antitrypsin augmentation therapy in the treatment of patients with alpha-1-antitrypsin deficiency. Biologics 3:193–204

Selvarasu S, Ow DS, Lee SY, Lee MM, Oh SK, Karimi IA, Lee DY (2009) Characterizing *Escherichia coli* DH5alpha growth and metabolism in a complex medium using genome-scale flux analysis. Biotechnol Bioeng 102(3):923–934

Sidorenko Y, Wahl A, Dauner M, Genzel Y, Reichl U (2008) Comparison of metabolic flux distributions for MDCK cell growth in glutamine- and pyruvate-containing media. Biotechnol Prog 24(2):311–320

Street JC, Delort AM, Braddock PS, Brindle KM (1993) A $^{1}H/^{15}N$ n.m.r. study of nitrogen metabolism in cultured mammalian cells. Biochem J 291(Pt 2):485–492

Teixeira AP, Santos SS, Carinhas N, Oliveira R, Alves PM (2008) Combining metabolic flux analysis tools and ^{13}C NMR to estimate intracellular fluxes of cultured astrocytes. Neurochem Int 52(3):478–486

Thorens B, Mueckler M (2010) Glucose transporters in the 21st century. Am J Physiol Endocrinol Metab 298(2):E141–E145

Wang Z, Ying Z, Bosy-Westphal A, Zhang J, Schautz B, Later W, Heymsfield SB, Muller MJ (2010) Specific metabolic rates of major organs and tissues across adulthood: evaluation by mechanistic model of resting energy expenditure. Am J Clin Nutr 92(6):1369–1377

Wittmann C, Heinzle E (2002) Genealogy profiling through strain improvement by using metabolic network analysis: metabolic flux genealogy of several generations of lysine-producing corynebacteria. Appl Environ Microbiol 68(12):5843–5859

Wlaschin KF, Hu WS (2007) Engineering cell metabolism for high-density cell culture via manipulation of sugar transport. J Biotechnol 131(2):168–176

Wurm FM (2004) Production of recombinant protein therapeutics in cultivated mammalian cells. Nat Biotechnol 22(11):1393–1398

Zwingmann C, Richter-Landsberg C, Leibfritz D (2001) ^{13}C isotopomer analysis of glucose and alanine metabolism reveals cytosolic pyruvate compartmentation as part of energy metabolism in astrocytes. Glia 34(3):200–212